Experimental Measurement of Gas Diffusivity in Bitumen: Results for Carbon Dioxide

ARTICLE *in* INDUSTRIAL & ENGINEERING CHEMISTRY RESEARCH · APRIL 2000

Impact Factor: 2.59 · DOI: 10.1021/ie990635a

2 AUTHORS, INCLUDING:

Anil K Mehrotra
The University of Calgary
160 PUBLICATIONS **2,347** CITATIONS

SEE PROFILE

Article

Experimental Measurement of Gas Diffusivity in Bitumen: Results for Carbon Dioxide

Simant R. Upreti, and Anil K. Mehrotra

Ind. Eng. Chem. Res., **2000**, 39 (4), 1080-1087• DOI: 10.1021/ie990635a • Publication Date (Web): 07 March 2000

Experimental Measurement of Gas Diffusivity in Bitumen: Results for Carbon Dioxide

Simant R. Upreti and Anil K. Mehrotra*

Department of Chemical and Petroleum Engineering, University of Calgary, Calgary, Alberta, Canada T2N 1N4

A new technique is developed to measure the diffusivity of gas in bitumen as a function of composition. Results are presented for a carbon dioxide−bitumen system, which is of considerable industrial relevance. The technique employs transient pressure data obtained from a nonintrusive pressure decay experiment at constant temperature and volume. The underlying theory is presented along with a computational algorithm to calculate diffusivity. Using experimental pressure decay data in the range 25−90 °C at 4 MPa, the diffusivity of carbon dioxide in bitumen is calculated. The results are compared with the limited data available in the literature. The approach is straightforward and can be easily applied to other nonvolatile liquid systems.

Introduction

Bitumen and heavy oil reserves in Canada[1] have a great potential to meet the future demand for petroleum products. An efficient in situ recovery from these reserves requires reduction in the bitumen viscosity which is very high, typically 100−1000 Pa s. Injection of light gases, such as nitrogen, methane, ethane, carbon monoxide, and carbon dioxide, causes reduction of bitumen viscosity.[2−5] As a result, these gases enhance recovery; therefore, knowledge of their diffusivity is essential for gas injection operations and reservoir simulation.[6]

Diffusivity is a transport property required to calculate the rate of mass transfer of a species because of molecular diffusion in a medium.[7] The statistical modeling of a large nonequilibrium system,[8] frequent in engineering, results in the *Fick's first law* which defines diffusivity as a ratio of medium-relative mass flux of a species to the negative of its concentration gradient along the flux. This ratio (also called Fick diffusivity), D, is related to the true transport property[9] called Maxwell−Stefan diffusivity,[10] $Đ$, as follows:

$$D = Đ \frac{\partial \ln a}{\partial \ln x} \equiv Đ\Gamma \tag{1}$$

In the above equation, a is the activity of the species, x is its mole fraction in the medium, and Γ is the thermodynamic nonideality factor which is related to concentration. Equation 1 indicates that (Fick) diffusivity should not be expected to be constant at a given temperature and pressure. Depending upon the nonideality, diffusivity of a species may vary with its concentration in the medium, with the effect being significant for dense gas and liquid systems.[11]

There are different experimental methods to measure the diffusivity of a gas in liquid. The direct method[12] involves compositional analysis of liquid samples extracted at different times. A class of indirect methods measures any change in property of medium brought about by the diffusing species and correlating the property with the composition. Such a property can be volume,[13] pressure,[14] solute volatilization rate,[15] position of the gas−liquid interface,[14,16] refraction of electromagnetic radiation,[17] etc. After the composition of the medium has been determined, a mass-transfer model is required to calculate the diffusivity. Another class of indirect methods[18] estimates the diffusivity from self-diffusion coefficients which are measured by devices such as NMR spectroscopy. For the direct method, extraction of samples is system-intrusive, and the estimation of dissolved gas in a sample is prone to experimental errors. Indirect methods based on property change have, until now, depended heavily on several simplifications in estimating the diffusivity value. Those based on self-diffusion coefficients are limited by the empirical mixing rules used to calculate the concentration-dependent diffusivity.

Unfortunately, little data are available for the diffusivity of gases in bitumen. Schmidt et al.[12] have reported the diffusivity of carbon dioxide in Athabasca bitumen using the direct method. They found that the diffusivity was concentration-dependent and the assumption of constant diffusivity in their calculations was not supported by the experiments. Zhang et al.[19] have calculated the diffusivity of carbon dioxide in heavy oil using the indirect method of pressure decay. They assumed diffusivity to be independent of concentration and no volume change of mixing. Nyugen and Farouq Ali[20] have used the direct method to calculate diffusivity of carbon dioxide when mixed with nitrogen. Mehrotra et al.[21] have examined various semiempirical correlations to predict diffusivity of carbon dioxide in bitumen using a corresponding states method. Das and Butler[16] have reported diffusivity of propane in Peace River bitumen in their vapor extraction process experiments using the height of the vapor−bitumen interface along with empirical correlations relating diffusivity with bitumen viscosity and composition. Their results also indicate a strong dependence of gas diffusivity on its concentration in bitumen.

In this paper, we report a nonintrusive method to determine gas diffusivity as a function of its concentration in bitumen and apply that to the carbon dioxide−bitumen system. Our method is indirect and measures

* Author to whom correspondence should be addressed. Phone: +1(403)220-7406. Fax: +1(403)284-4852. E-mail: mehrotra@ucalgary.ca.

10.1021/ie990635a CCC: $19.00
Published on Web 03/07/2000

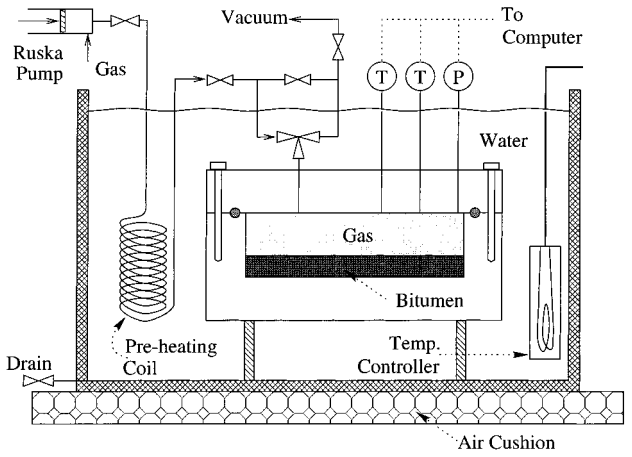

Figure 1. Schematic diagram of the experimental apparatus.

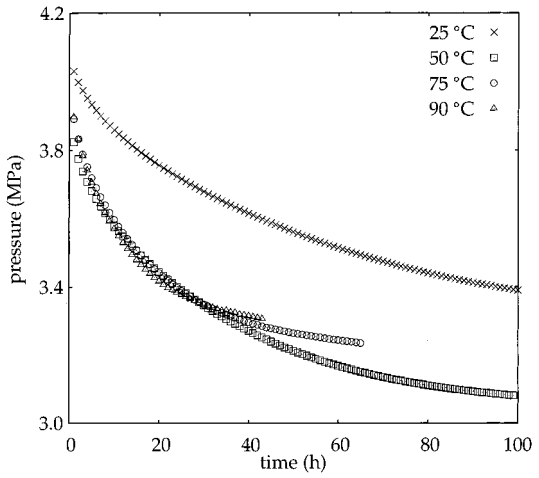

Figure 2. Experimental pressure decay (recorded every 90 s) plotted every hour for different temperatures at an initial pressure of approximately 4 MPa.

change in pressure with time as the gas diffuses into bitumen. It utilizes a comprehensive distributed parameter model of mass transfer and employs a functional optimization technique to compute the concentration-dependent gas diffusivity. The calculation technique does not depend on empirical correlations. It incorporates the variation in the density of the gas−liquid mixture. It evaluates the initial interfacial equilibrium composition from the recorded pressure data and optimizes it further.

Experimental Setup

Figure 1 shows a schematic diagram of the experimental setup. The apparatus was conservatively designed[22] through mathematical modeling and simulation of the pressure decay experimentation based on a predictive model of gas diffusivity in bitumen. The pressure decrease is recorded as gas diffuses into a layer of bitumen underneath inside a closed vessel kept at constant temperature.

The experimental apparatus comprises a 10-cm-diameter cylindrical pressure vessel of depth 3 cm, which holds the gas and bitumen. A Teflon O ring between the base and lid of the vessel secures the vessel leak-proof with the help of 10 threaded bolts. A Ruska pump supplies the gas at the desired pressure into the vessel via a preheating coil. So that the incoming gas may not disturb the flat bitumen surface, a tiny baffle is provided at the base of the lid at the gas entry point. A vacuum pump is used for purging. Two thermocouples indicate the temperature of the gas and bitumen phases. The heart of the apparatus is a Paroscientific Digiquartz Intelligent pressure transmitter. A high resolution of ±0.13 Pa is achieved by its special quartz crystal resonator whose frequency of oscillation varies with pressure-induced stress. Quartz crystal sensors are successfully used in such diverse fields as hydrology, aerospace, meteorology, oceanography, process control, energy exploration, and laboratory instrumentation. Connected with the thermocouples and the pressure sensor is a computer which displays and records the data online. A Haake temperature controller/circulator maintains the desired temperature of a water bath which sits on an air cushion. The preheating coil and the pressure vessel are submerged entirely in the water bath.

Experimental Procedure

Before the experiments were started, the vessel was pressurized with gas and leak-tested several times at constant temperature in the range 4−8 MPa and 25−90 °C. No gas leak was detected by the pressure sensor for 7 days with the application of (i) silicon high-vacuum grease on the Teflon O ring, (ii) torque of 68 N m on each threaded bolt, and (iii) a gas pressure, equal to the pressure inside the vessel, on both side ports of the three-way valve on the vessel. The gas chromatograph analyses of the gas samples extracted from the vessel after purging (five times successive introduction and withdrawal of gas into and from the empty vessel) confirmed the absence of air. The following experimental procedure was implemented:

A. Gradually pour bitumen into the vessel such that it forms a horizontal surface layer free of air bubbles of approximately 1 cm thick. Record the mass of bitumen.

B. Apply silicon high-vacuum grease on the Teflon O ring. Bolt the lid on the vessel with a uniform torque of 68 N m.

C. Place the vessel inside the constant-temperature water bath. Secure remaining connections on the three-way valve and the sensors. Start the online display of the vessel pressure and temperature.

D. Purge the air from the vessel after the bitumen attains the bath temperature. This was done by repeatedly introducing the test gas into the vessel at atmospheric pressure and applying vacuum six times.

E. Introduce additional gas to achieve the desired pressure and shut off the three-way valve. Immediately, start recording the vessel pressure. Gas-pressurize the two side ports of the three-way valve to the vessel's internal start-up pressure.

F. Terminate pressure recording when the pressure decay falls below the resolution of pressure sensor, i.e., ±0.13 Pa (usually after 2−6 days). Collect gas samples for GC analysis.

G. Open the vent line and slowly depressurize the vessel to atmospheric pressure. Detach the vessel from the bath. Open and clean up the vessel for the next experiment.

A complete set of pressure decay data for the carbon dioxide−bitumen system at 4 MPa is plotted in Figure 2. Carbon dioxide of 99.998% purity, supplied by Praxair, was used in the experiments. The source of bitumen was "Suncor Coker Feed" obtained from the Sample Bank of Alberta Research Council, Edmonton, Alberta, Canada. Before using in the experiments, it was extracted with toluene to remove water and solids and recovered in a

Table 1. Analysis of the Athabasca Bitumen Sample Used

substance	mass fraction
carbon	0.8384
hydrogen	0.0970
nitrogen	0.0054
sulfur	0.0474
asphaltenes	0.1730
400 °C distillate	0.1980
400 °C residue	0.6290

	θ (°C)			
	25	80	95	110
ρ_b (kg m^{-3})	1006.6			
μ_b (Pa s)		0.767	0.320	0.143

rotary evaporator under vacuum. Table 1 shows the analysis of the bitumen used in the experiments.

Theoretical Development

As shown in Figure 2, the diffusion of gas into bitumen decreases the system pressure. Because bitumen is nondiffusing, the recorded pressure versus time data, the *PVT* relationship of the gas, and the density data of the gas−bitumen mixture yield, at time t, the experimental mass of gas absorbed in the bitumen phase. The primary objective is to find the gas diffusivity, D, at gas concentration $c(z,t)$ at depth z and time t in the bitumen phase such that the mass of gas absorbed, calculated from a pertinent mass-transfer model, becomes equal to its experimental value.

Mass-Transfer Model. The process of mass transfer in our experiments satisfies the following conditions:

A. There is no mass transfer of bitumen into the gas phase.

(i) The bitumen used in our experiments is highly nonvolatile. A SIMDIST analysis showed that less than 1% of it volatilizes at atmospheric pressure and a temperature less than 200 °C. In fact, no bitumen fractions were detected in the GC analyses of gas samples extracted after the completion of experiments conducted in the range 25−90 °C.

B. Mass transfer of gas into bitumen is solely due to molecular diffusion.

(i) The chance of thermally induced convection currents in the bitumen phase can be precluded because the temperature of the pressure vessel was kept uniformly constant within ±0.1 °C.

(ii) Because the dissolution of carbon dioxide does not increase the bitumen density, there is no possibility, whatsoever, of density-induced convection currents in the bitumen phase.

(iii) Other than the water circulator suspended from an isolated frame, there was no rotating or vibrating equipment in the experimental apparatus. To avoid any effect of external vibrations, the apparatus was placed over air cushions.

C. The concentration gradient is only along the depth of the bitumen layer, i.e., the z direction.

(i) This arises from the symmetry of the system.

D. There are no chemical reactions.

(i) The absorption of gas in bitumen is a purely physical phenomenon.

Under the aforementioned conditions, the equation of continuity for the gas diffusing into the bitumen phase can be written as

$$\frac{\partial c}{\partial t} = D\left[1 + \frac{c}{\rho_b}\right]\frac{\partial^2 c}{\partial z^2} + \left[\left(1 + \frac{c}{\rho_b}\right)\frac{\partial D}{\partial c} + \frac{D}{\rho_b}\right]\left(\frac{\partial c}{\partial z}\right)^2 \equiv f \quad (2)$$

At constant temperature, D is considered to be a function of gas concentration in the bitumen phase but independent of pressure during an experimental run (results presented later justify these assumptions). Initially there is no gas in bitumen, i.e.,

$$c(z,0) = 0 \qquad \forall z: \quad 0 < z \le L \quad (3)$$

The interfacial gas concentration is always known, i.e.,

$$c(0,t) = c_{sat}(t) \qquad \forall t: \quad 0 \le t \le T \quad (4)$$

Because there is no mass transfer at the bottom of the vessel,

$$\left.\frac{\partial c}{\partial z}\right|_{z=L} = 0 \qquad \forall t: \quad 0 \le t \le T \quad (5)$$

Equations 3−5 are the initial and boundary conditions for eq 2.

The Objective. Mathematically, the objective functional can be written as

$$\underset{\min}{I} = \int_0^T \int_0^L F(z,t)\, \mathrm{d}z\, \mathrm{d}t \quad (6)$$

where

$$F(z,t) = \left[1 - \frac{c(z,t)}{c_{exp}}\right]^2 \quad (7)$$

Here, I is the objective functional panning the depth of bitumen layer, $0 \le z \le L$, and the run time, $0 \le t \le T$. c and c_{exp} are respectively the calculated and experimental values of the mass of gas dissolved per unit volume of the bitumen phase. I is related to the root-mean-squared relative error, I_{rms}, with respect to the mass of gas absorbed in bitumen:

$$I_{rms} = \sqrt{\frac{1}{T}\int_0^T \left[1 - \frac{m_{g,abs}}{m_{g,exp}}\right]^2 \mathrm{d}t} = \frac{1}{L}\sqrt{\frac{I}{T}} \quad (8)$$

During numerical minimization of I, which is presented later, the time integral in eq 6 ensures diffusivity calculation for a maximum number of distinct concentration values in the overall range of gas concentration in the bitumen phase. At the minimum value of I, the experimental mass of dissolved gas, $m_{g,exp}$, would tend to its calculated value, $m_{g,abs}$, that is given by

$$m_{g,abs}(t) = \frac{\pi d^2}{4}\int_0^L c(z,t)\, \mathrm{d}z \quad (9)$$

In the above equation, $c(z,t)$ is the gas concentration in the bitumen phase at any time t and depth z, and d is the internal diameter of the pressure vessel. $c(z,t)$ is calculated using the equation of continuity for gas in the bitumen phase

$$G(z,t) = \frac{\partial c}{\partial t} - f\left(c, \frac{\partial c}{\partial z}, \frac{\partial^2 c}{\partial z^2}, D\right) = 0 \quad (10)$$

Equation 10 is the optimization constraint for eq 6. In

addition to the gas diffusivity D, we also consider the interfacial concentration of gas at the final time, $c(0,T)$ ($\equiv c_{sat}(T)$) as an optimization variable.

Equation 10 is a *nonholonomic* condition because G is a highly nonlinear partial differential equation, the boundary condition of which (eq 4) is a set of discrete values. Therefore, for the solution, we need an adjoint variable, $\lambda(z,t)$, which incorporates the constraint of eq 10 into eq 6 to yield an augmented objective functional[23]

$$\min_{J} = \int_0^T \int_0^L [F(z,t) + \lambda(z,t)\, G(z,t)]\, \mathrm{d}z\, \mathrm{d}t \qquad (11)$$

The problem now becomes equivalent to the minimization of J.

Optimality Criterion. To derive the necessary optimality conditions, we perturb F and G as follows:

$$\delta F = \frac{\partial F}{\partial c}\,\delta c \qquad (12)$$

$$\delta G = \frac{\partial(\delta c)}{\partial t} - \frac{\partial f}{\partial c}\,\delta c - \frac{\partial f}{\partial \dot{c}}\,\delta \dot{c} - \frac{\partial f}{\partial \ddot{c}}\,\delta \ddot{c} - \frac{\partial f}{\partial D}\,\delta D \qquad (13)$$

Substituting eqs 12 and 13 into eq 11 gives the following first variation in J:

$$\delta J = \int_0^T \int_0^L [\delta F(z,t) + \lambda\, \delta G]\, \mathrm{d}z\, \mathrm{d}t$$
$$= \int_0^T \int_0^L \left[\left\{\frac{\partial F}{\partial c} - \lambda \frac{\partial f}{\partial c}\right\} \delta c + \lambda\left\{\frac{\partial(\delta c)}{\partial t} - \frac{\partial f}{\partial \dot{c}}\,\delta \dot{c} - \frac{\partial f}{\partial \ddot{c}}\,\delta \ddot{c} - \frac{\partial f}{\partial D}\,\delta D\right\}\right] \mathrm{d}z\, \mathrm{d}t \qquad (14)$$

Integration by parts of the third, fourth and fifth terms of the above equation yields

$$\int_0^T \int_0^L \lambda \frac{\partial(\delta c)}{\partial t}\, \mathrm{d}z\, \mathrm{d}t = \int_0^L \left\{\left[\lambda\, \delta c\right]_0^T - \int_0^T \frac{\partial \lambda}{\partial t}\, \delta c\, \mathrm{d}t\right\} \mathrm{d}z \qquad (15)$$

$$\int_0^T \int_0^L \lambda \frac{\partial f}{\partial \dot{c}}\, \delta \dot{c}\, \mathrm{d}z\, \mathrm{d}t = \int_0^T \left\{\left[\lambda \frac{\partial f}{\partial \dot{c}}\, \delta c\right]_0^L - \int_0^L \frac{\partial}{\partial z}\left(\lambda \frac{\partial f}{\partial \dot{c}}\right) \delta c\, \mathrm{d}z\right\} \mathrm{d}t \qquad (16)$$

$$\int_0^T \int_0^L \lambda \frac{\partial f}{\partial \ddot{c}}\, \delta \ddot{c}\, \mathrm{d}z\, \mathrm{d}t = \int_0^T \left\{\left[\lambda \frac{\partial f}{\partial \ddot{c}} \frac{\partial(\delta c)}{\partial z} - \frac{\partial}{\partial z}\left(\lambda \frac{\partial f}{\partial \ddot{c}}\right) \delta c\right]_0^L + \int_0^L \frac{\partial^2}{\partial z^2}\left(\lambda \frac{\partial f}{\partial \ddot{c}}\right) \delta c\, \mathrm{d}z\right\} \mathrm{d}t \qquad (17)$$

Substitution of the above expressions into eq 14 results in

$$\delta J = \int_0^T \int_0^L \left\{-\frac{\partial \lambda}{\partial t} + \frac{\partial F}{\partial c} - \lambda \frac{\partial f}{\partial c} + \frac{\partial}{\partial z}\left(\lambda \frac{\partial f}{\partial \dot{c}}\right) - \frac{\partial^2}{\partial z^2}\left(\lambda \frac{\partial f}{\partial \ddot{c}}\right)\right\} \delta c\, \mathrm{d}z\, \mathrm{d}t - \int_0^T \int_0^L \lambda \frac{\partial f}{\partial D}\, \delta D\, \mathrm{d}z\, \mathrm{d}t +$$
$$\int_0^L \left[\lambda\, \delta c\right]_0^T \mathrm{d}z + \int_0^T \left[\lambda \frac{\partial f}{\partial \dot{c}} - \frac{\partial}{\partial z}\left(\lambda \frac{\partial f}{\partial \ddot{c}}\right)\right]_{z=0} \delta c(0,t)\, \mathrm{d}t -$$
$$\int_0^T \left[\lambda \frac{\partial f}{\partial \dot{c}} - \frac{\partial}{\partial z}\left(\lambda \frac{\partial f}{\partial \ddot{c}}\right)\right]_{z=L} \delta c(L,t)\, \mathrm{d}t - \int_0^T \left[\lambda \frac{\partial f}{\partial \ddot{c}} \frac{\partial(\delta c)}{\partial z}\right]_0^L \mathrm{d}t \qquad (18)$$

We now simplify eq 18.

1. The third integral in eq 18 is eliminated as follows:

(i) The initial concentration of gas in bitumen, $c(z,0)$, is known at the interface and is zero everywhere in the interval $0 < z \le L$. Because $c(z,0)$ is overall specified, its variation is ruled out, i.e.,

$$\delta c(z,0) = 0 \quad \forall z: \quad 0 \le z \le L \qquad (19)$$

(ii) The final concentration of gas in bitumen, $c(z,T)$, in the interval $0 < z \le L$ is not specified. Variation due to $c(z,t)$ is eliminated if its multiplicative term, $\lambda(z,T)$, in the third integral of eq 18 is set to zero, i.e.,

$$\lambda(z,T) = 0 \qquad \forall z: \quad 0 < z \le L \qquad (20)$$

(iii) Because the equilibrium concentration of gas at the interface, $c(0,T)$, is an optimization variable, it can vary. To eliminate its variation, we set its multiplicative term, $\lambda(0,T)$ to zero. Therefore, in combination with eq 20,

$$\lambda(z,T) = 0 \qquad \forall z: \quad 0 \le z \le L \qquad (21)$$

2. The equilibrium concentration of gas at the interface, $c(0,t)$ ($\equiv c_{sat}(t)$), is specified in the interval $0 \le t < T$ (eq 33) and, thus, it cannot vary. Hence,

$$\delta c(0,t) = 0 \qquad \forall t: \quad 0 \le t < T \qquad (22)$$

At the final time T, the application of eq 21 sets the multiplicative term of $\delta c(0,t)$ in the fourth integral in eq 18 to zero. As a result, the fourth integral gets eliminated altogether.

3. To eliminate the fifth integral in eq18, we force the following multiplicative term in the integrand to zero:

$$\left[\lambda \frac{\partial f}{\partial \dot{c}} - \frac{\partial}{\partial z}\left(\lambda \frac{\partial f}{\partial \ddot{c}}\right)\right]_{z=L} = 0 \qquad (23)$$

4. To eliminate the sixth integral in eq 18, we force the following multiplicative term in the integrand to zero:

$$\left[\lambda \frac{\partial f}{\partial \ddot{c}}\right]_{z=0,L} = 0 \qquad (24)$$

5. Finally, with the following definition of λ:

$$-\frac{\partial \lambda}{\partial t} + \frac{\partial F}{\partial c} - \lambda \frac{\partial f}{\partial c} + \frac{\partial}{\partial z}\left(\lambda \frac{\partial f}{\partial \dot{c}}\right) - \frac{\partial^2}{\partial z^2}\left(\lambda \frac{\partial f}{\partial \ddot{c}}\right) = 0 \qquad (25)$$

and the application of eq 24, the first integral in eq 18 gets reduced to

$$\int_{T-\mathrm{d}t}^{T} \int_0^{\mathrm{d}z} \frac{\partial F}{\partial c}\, \delta c\, \mathrm{d}z\, \mathrm{d}t \qquad (26)$$

Equations 21, 23, and 24 form the natural constraints for eq 25. Application of eqs 19−25 reduces eq 18 to

$$\delta J = \int_{T-\mathrm{d}t}^{T} \int_0^{\mathrm{d}z} \frac{\partial F}{\partial c}\, \delta c\, \mathrm{d}z\, \mathrm{d}t - \int_0^T \int_0^L \lambda \frac{\partial f}{\partial D}\, \delta D\, \mathrm{d}z\, \mathrm{d}t \qquad (27)$$

At the minimum, the first variation of J given by the above equation is zero. In order for D and $c(0,T)$ to be minimal, $\delta J \ge 0$ for all possible small variations δD and $\delta c(0,T)$. That is only possible when

$$\lambda \frac{\partial f}{\partial D} \equiv J_D = 0 \qquad \forall z,t: \quad 0 \le z \le L, \quad 0 \le t \le T \qquad (28)$$

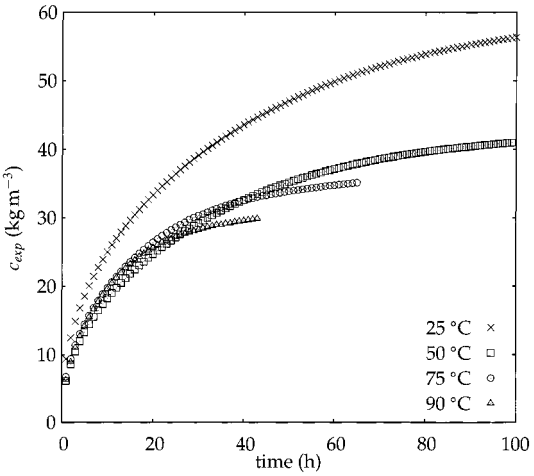

Figure 3. Mass of CO_2 absorbed in bitumen per unit mixture volume plotted every hour for different temperatures at 4 MPa.

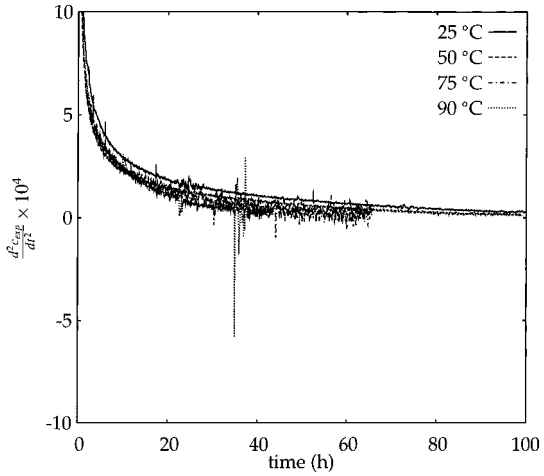

Figure 4. Second time derivative of the mass of CO_2 absorbed per unit volume in bitumen at 4 MPa and different temperatures.

and

$$\frac{\partial F}{\partial c} \equiv J_{c(0,T)} = 0, \quad z = 0, \quad t = T \tag{29}$$

Thus, eqs 28 and 29 are the necessary conditions for the minimum of J. In these equations, J_i is called the variational derivative of J with respect to i. Its negative value is the direction of the steepest descent of J in its function space of z and t.

Diffusivity Calculation

To calculate gas diffusivity, in addition to the above relations, we need a model for the density of the gas−bitumen mixture, ρ_{mix}. It is required to calculate (i) the experimental mass of gas absorbed per unit volume of the bitumen layer, $c_{exp}(t)$, and (ii) the interfacial gas concentration, $c(0,t)$.

The Model for ρ_{mix}. A linear least-squares method was used to fit the published experimental data[2−5] on the carbon dioxide−bitumen system for several samples of bitumen into the following simple equation:

$$\rho_{mix} = \rho_{b@25\ °C}(1.2011 - 6.6506 \times 10^{-4}\theta - 5.0387 \times 10^{-2}w); \quad 20 \le \theta \le 200, \quad 0.0072 \le w \le 0.0922 \tag{30}$$

with a fit standard error of 0.0152, r^2 coefficient of determination value of 0.8171, its degree of freedom adjusted value of 0.8106, and an F statistic of 189.86. In eq 30, θ is temperature in degrees Celsius and w is the mass fraction of carbon dioxide absorbed in bitumen. ρ_{mix} for the carbon dioxide−bitumen system was found to be independent of pressure and does not increase with w.

Calculation of c_{exp}. The following iterative scheme was developed for the sequential calculation of c_{exp} from pressure readings sampled at a regular time interval of τ in seconds:

1. $t = 0$
2. $m_{g,exp}(0) = 0$
3. $m_g(0) = [M_g P(0)\ V_g(0)]/[Z(0)\ R(\theta + 273.15)]$
4. $w(t+\tau) = [100 m_{g,abs}(t)]/[m_{g,exp}(t) + m_b]$
5. $\rho_{mix}(t+\tau) = \rho_{b@25\ °C}[1.0159 - 6.657 \times 10^{-4}\theta - 3.5574 \times 10^{-4}w(t)]$
6. $V_g(t+\tau) = V_T - [m_b + m_{g,exp}(t)]/[\rho_{mix}(t)]$
7. $m_g(t+\tau) = [M_g P(t)\ V_g(t)]/[Z(t)\ R(\theta + 273.15)]$
8. $m_{g,exp}(t+\tau) = m_g(0) - m_g(t+\tau)$
9. $c(t+\tau) = m_g(t)/V_g(t)$
10. $L(t+\tau) = [m_b + m_{g,exp}(t)]/[\rho_{mix}(t)\ (\pi d^2/4)]$
11. $c_{exp}(t+\tau) = [m_{g,exp}(t+\tau)]/[(\pi d^2/4)L(t+\tau)]$
12. $t = t + \tau$
13. go back to step 4 until $t = T$

Note that the compressibility factor, Z, was calculated from the experimental PVT data[24] of carbon dioxide. Figure 3 shows the plot of calculated c_{exp} values corresponding to the pressure decay data in Figure 2.

Calculation of $c(0,t)$. The estimation of interfacial gas concentration is based on the following experimental observations:

1. Time derivatives of c_{exp} of orders higher than 2 are insignificant. For the experiments performed, Figure 4 shows the second time derivative of c_{exp} that becomes nearly constant toward the terminal time T. Therefore,

$$\frac{dc_{exp}}{dt} = \left.\frac{d^2c_{exp}}{dt^2}\right|_{t=T} t + \psi_1 \qquad \forall t: \quad t \ge T \tag{31}$$

where

$$\psi_1 = \left[\frac{dc_{exp}}{dt} - t\frac{d^2c_{exp}}{dt^2}\right]_{t=T} \tag{32}$$

2. Experimental gas-solubility data for several bitumens[2−5] show that, at $P < P_c$, c_{sat} is linearly related with the system pressure, P, which implies that

$$\frac{1}{P}\frac{dP}{dt} = \frac{1}{c_{sat}}\frac{dc_{sat}}{dt} \tag{33}$$

At some time $T_\infty > T$, when bitumen would get completely saturated with gas, the pressure differential with respect to time would be zero. From eq 31

$$T_\infty = -\psi_1\left[\left(\frac{d^2c_{exp}}{dt^2}\right)^{-1}\right]_{t=T} \tag{34}$$

Integration of eq 31 from time T to T_∞ yields c_{exp} at T_∞ which is the saturation concentration c_{sat} at that time.

For an initial estimate of the optimization variable c_{sat} at time T, we integrate the equation

$$\frac{dc_{sat}}{dt} = \frac{d^2c_{sat}}{dt^2}\, t + \psi_2 \tag{35}$$

backward, from time T_∞ to T, utilizing eq 33. In eq 35, ψ_2 is a constant given by

$$\psi_2 = \left[\frac{dc_{sat}}{dt} - t\,\frac{d^2c_{sat}}{dt^2}\right]_{t=T} \tag{36}$$

c_{sat} for time $0 \le t < T$ is calculated from eq 33 and c_{sat} at time T. Figure 5 shows the plots of optimal interfacial carbon dioxide concentration with time for different temperatures at 4 MPa.

Adjoint Equation. Using eqs 2 and 7, eq 25 can be written as

$$\frac{\partial\lambda}{\partial t} + \frac{2}{c}\left[1 - \frac{c}{c_{exp}}\right] - \frac{\lambda}{\rho_b}\frac{\partial D}{\partial c}\left(\frac{\partial c}{\partial z}\right)^2 - \lambda\left[1 + \frac{c}{\rho_b}\right]\frac{\partial D}{\partial c}\frac{\partial^2 c}{\partial z^2} - \lambda\left[1 + \frac{c}{\rho_b}\right]\frac{\partial^2 D}{\partial c^2}\left(\frac{\partial c}{\partial z}\right)^2 + D\left[1 + \frac{c}{\rho_b}\right]\frac{\partial^2\lambda}{\partial z^2} = 0 \tag{37}$$

for which eq 21 is the initial condition. Equations 2, 5, and 23 yield

$$\left.\frac{\partial\lambda}{\partial z}\right|_{z=L} = 0 \qquad \forall t:\ \ 0 \le t \le T \tag{38}$$

Equations 2 and 24 give

$$\lambda(0,t) = \lambda(L,t) = 0 \qquad \forall t:\ \ 0 \le t \le T \tag{39}$$

Note that eqs 38 and 39 are the boundary conditions for eq 37.

Solution Methodology. Because eqs 2 and 37 are nonlinear and the interfacial gas concentration, given by eq 4, is a set of discrete experimental values, an analytical solution is not possible. We used the following numerical algorithm to calculate optimal $D(c)$ by iterative minimization of J:

1. Initialize $D(c)$ and $c(0,T)$.
2. Solve eq 2 forward in time along with eqs 3−5.
3. Solve eq 37 backward in time along with eqs 21, 38, and 39.
4. To minimize J, apply the gradient corrections in $D(c)$ given by

$$\Delta D(c_0) = \frac{\epsilon_1}{T}\int_0^T J_D(c_0)\, dt, \qquad \forall c_0:\ \ 0 \le c_0 \le c_{max} \equiv c(0,0) \tag{40}$$

Repeat steps 2 and 3 and apply the following gradient correction in $c(0,T)$:

$$\Delta c(0,T) = -\frac{\epsilon_2}{T}\, J_{c(0,T)} \tag{41}$$

Note that ϵ_1 and ϵ_2 are positive relaxation parameters which scale the correction to the order of magnitude of the optimization variable.

5. Go to step 2 until either I or ΔD as well as $\Delta c(0,T)$ become negligibly small.

Numerical Solution. $D(c)$ was initialized with a constant value. $c_{sat}(T)$ was estimated using eq 35, and the rest of its values were calculated from eq 33. Equations 2 and 37 were written in a finite-difference form in the z direction. They were integrated using an adaptive step size control method of Bulirsch and Stoer.[25] The solutions obtained for these equations are smooth and nonsingular. For such cases, this method is well-known for very efficient and high-accuracy solutions.[26] With an accuracy of 1×10^{-4} in the time domain, the number of grid points along the z direction, N, was increased and fixed at 32 when the corresponding change in the solution was found to be negligible.

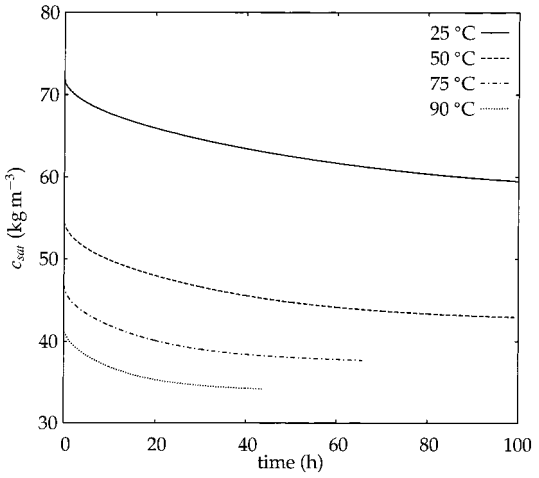

Figure 5. Optimal interfacial concentration of CO_2 in bitumen versus time at 4 MPa and different temperatures.

To refine $D(c)$ and $c_{sat}(T)$, we used the method of conjugate gradients.[27] As shown in eq 40, differential changes were averaged for diffusivity at any concentration which had multiple existence in the time domain. This strategy has an underlying assumption that, during the experiment, diffusivity at a given concentration did not change with pressure. It is validated by very low optimal values of I_{rms} in all of the calculations.

It may be noted that high gas concentrations exist only near the interface and the final time when $\lambda = 0$ (refer eqs 21 and 39). Hence, close to the optimum, λ tends to zero near the interface and the final time. This would hinder, for higher gas concentrations, further refinements in D given by eq 40. To achieve a very low value of J, we initialized $D(c)$ with a value high enough to yield the lowest possible value of I_{rms} that would keep $c \le c_{exp}$ at all t. This is the minimum if the diffusivity is assumed to be independent of concentration.

In Figure 6, the initial and optimal values of diffusivity, the saturation mass fraction of carbon dioxide, and its absorbed mass in bitumen at 4 MPa and 25 °C are presented. With the iterative refinement in $D(c)$ and c_{sat}, the I_{rms} value decreases monotonically to a low value of 2.2×10^{-2}. That is the optimal point when the gradient corrections of eqs 40 and 41 tend to zero and no further improvement is possible. The experimental and the optimally calculated values of m_g are observed to match very well.

A sensitivity analysis on the optimal diffusivity values was undertaken by varying the density and the gas solubility. For ±1% change in experimental ρ_{mix} and c_{sat}, Figure 7 shows the diffusivity values at 4 MPa and 25 °C. Maximum change in the diffusivity value occurs near the peak and is less than 5%. Similar results were obtained for other temperatures.

Results

Figure 8 presents the diffusivity results for the carbon dioxide−bitumen system in the range 25−90 °C at 4

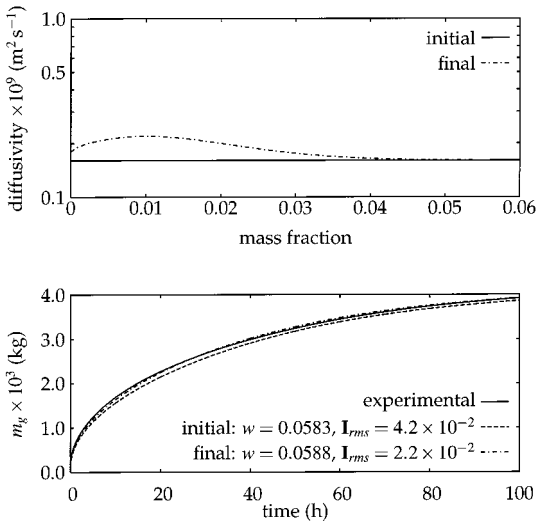

Figure 6. Initial and final values of diffusivity and mass of CO_2 absorbed in bitumen at 4 MPa and 25 °C.

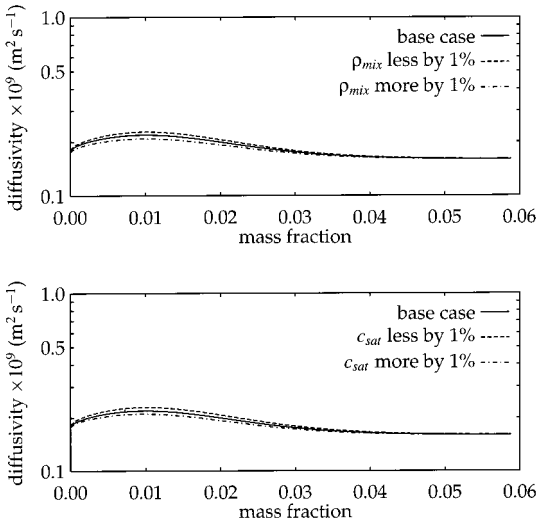

Figure 7. Sensitivity analysis on diffusivity of CO_2 in bitumen at 4 MPa and 25 °C with respect to ρ_{mix} and c_{sat}.

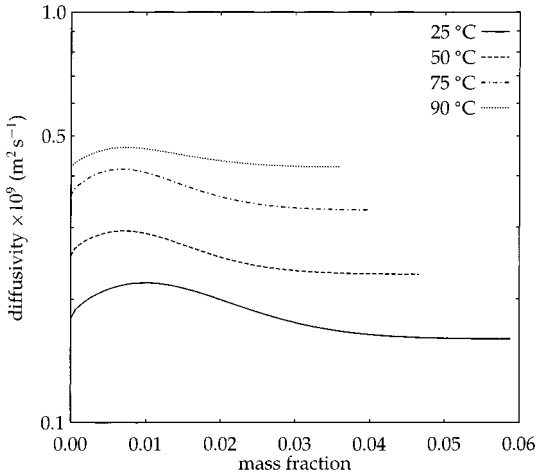

Figure 8. Diffusivity of CO_2 in bitumen at 4 MPa and different temperatures.

MPa. As shown in Figure 8, at a given temperature, the diffusivity of carbon dioxide varies with its concentration in bitumen. The diffusivity increases with the gas mass fraction until it attains a maximum value. It then decreases and levels off at the gas-solubility value that is governed by the interfacial gas concentration at the experimental pressure and temperature conditions.[2−5] The peak values of diffusivity lie in the mass fraction range of 0.007−0.010.

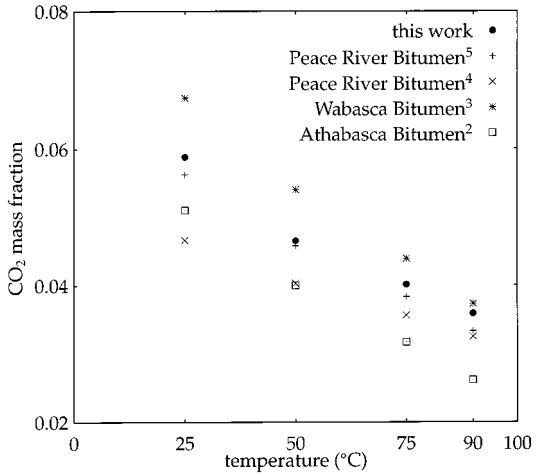

Figure 9. Solubility of CO_2 in bitumen at 4 MPa and different temperatures.

Table 2. Comparison of Carbon Dioxide Diffusivity with Other Published Results

source of data	crude oil/bitumen	P (MPa)	θ (°C)	$D \times 10^9$ (m^2 s^{-1})
ref 12	Athabasca bitumen	4.8−4.9	19.5−20	0.16−1.21
ref 19	heavy oil	2.843	21	4.76
ref 20	Aberfeldy oil	1	23	6
ref 21	Athabasca bitumen	*a*	23	5.17 (predicted)
this work	Athabasca bitumen	4	25−90	0.16−0.47

[a] At 0.4 mole fraction of carbon dioxide (corresponds to the maximum value of w in this work).

For a given value of carbon dioxide concentration in bitumen, the diffusivity is found to increase with temperature. With an increase in temperature from 25 to 90 °C, diffusivity increases approximately twofold. The peak value increases from 2.2×10^{-10} m^2 s^{-1} at 25 °C to 4.7×10^{-10} m^2 s^{-1} at 90 °C.

Figure 9 compares the gas solubility, i.e., the optimal saturated mass fraction of carbon dioxide in bitumen, with experimental values for different bitumens at 4 MPa and different temperatures.[2−5] The optimal values calculated in this work are in good agreement with the experimental carbon dioxide solubilities in bitumen.

Table 2 compares our carbon dioxide diffusivity results with those of other investigators. For similar pressure and temperature conditions, the values of carbon dioxide diffusivity are observed to lie in the same range.

Conclusions

A new technique based on pressure decay experimentation has been developed for the measurement of concentration-dependent gas diffusivity in bitumen. This technique is used to determine the diffusivity of carbon dioxide in Athabasca bitumen in the range 25−90 °C at 4 MPa. An algorithm based on functional minimization is developed to compute diffusivity as a function of the gas concentration in bitumen. It also enables the determination of gas solubility from the

same experiment. The technique can be readily applied to determine the gas diffusivity in other nonvolatile liquids.

The diffusivity of carbon dioxide in bitumen is found to be a unimodal function of its concentration in bitumen. This is plausible as the gas molecules reduce bitumen viscosity and are expected to facilitate molecular diffusion of gas until after attaining a certain concentration threshold beyond which their concentration hampers further diffusion.

The results also indicate that, at a pressure of 4 MPa, the diffusivity at a given carbon dioxide concentration increases with temperature which is normal.

Acknowledgment

Financial support was provided by the Natural Sciences and Engineering Research Council (NSERC) of Canada and the Department of Chemical and Petroleum Engineering, University of Calgary.

Nomenclature

c = calculated concentration of gas in bitumen (kg m^{-3})
c_{exp} = experimental mass of gas absorbed in bitumen per unit mixture volume (kg m^{-3})
c_{sat} = saturated concentration of gas in bitumen (kg m^{-3})
d = internal diameter of the pressure vessel (0.1 m)
I = objective functional
I_{rms} = root-mean-squared relative error
J = augmented objective functional
L = thickness of the bitumen layer (m)
m_b = mass of bitumen (kg)
m_g = mass of gas in the gas phase (kg)
$m_{g,abs}$ = calculated mass of gas absorbed in the bitumen layer (kg)
$m_{g,exp}$ = experimental mass of gas absorbed in the bitumen layer (kg)
M_g = molar mass of gas (kg kmol^{-1})
P = pressure (Pa)
P_c = critical pressure (Pa)
R = universal gas constant (8314 J kmol^{-1} K^{-1})
t = time (s)
T = total experimental run time (s)
V_T = total volume of the pressure cell (2.3562×10^{-4} m^3)
V_g = volume of the gas phase in the pressure cell (m^3)
w = mass fraction of gas in bitumen
z = depth in the bitumen layer (m)
Z = compressibility factor
D = (Fick) diffusivity of gas in bitumen (m^2 s^{-1})
D = Maxwell−Stefan diffusivity (m^2 s^{-1})
μ_b = viscosity of bitumen (Pa s)
ρ_b = density of bitumen (kg m^{-3})
$\rho_{b@25\ °C}$ = density of bitumen at 25 °C (kg m^{-3})
ρ_{mix} = density of the gas−bitumen mixture (kg m^{-3})
τ = sample time (90 s)
θ = temperature (°C)
λ = adjoint variable

Literature Cited

(1) Allen, F. H. The Canadian Oil Sands: A Race Against the Clock. 1st UNITAR Conference, Edmonton, Alberta, June 4−12, 1979. In *The Future of Heavy Oils and Tar Sands*; McGraw Hill Book Company: New York, 1981.

(2) Svrcek, W. Y.; Mehrotra, A. K. Gas Solubility, Viscosity and Density Measurements for Athabasca Bitumen. *J. Can. Pet. Technol.* **1982**, *21* (4), 31−38.

(3) Mehrotra, A. K.; Svrcek, W. Y. Viscosity, Density and Gas Solubility Data for Oil Sand Bitumens. Part III: Wabasca Bitumen Saturated with N_2, CO, CH_4, CO_2 and C_2H_6. *AOSTRA J. Res.* **1985**, *2* (2), 83−93.

(4) Mehrotra, A. K.; Nighswander, J. A.; Kalogerakis, N. Data and Correlation for CO_2−Peace River Bitumen Phase Behaviour at 22−200 °C. *AOSTRA J. Res.* **1989**, *5* (4), 351−358.

(5) Mehrotra, A. K.; Svrcek, W. Y. Viscosity, Density and Gas Solubility Data for Oil Sand Bitumens. Part II: Peace River Saturated with N_2, CO, CH_4, CO_2 and C_2H_6. *AOSTRA J. Res.* **1985**, *1* (4), 269−279.

(6) Grogan, A. T.; Pinczewski, W. V. The Role of Molecular Diffusion Processes in Tertiary CO_2 Flooding. *J. Pet. Technol.* **1987**, *39* (5), 591−602.

(7) Lightfoot, E. N., Jr.; Lightfoot, E. J. Mass Transfer. In *Encyclopedia of Separation Technology*; Ruthven, D. M., Ed.; John Wiley & Sons: New York, 1997; Vol. 2, pp 1138−1147.

(8) Hirschfelder, J. O.; Curtiss, C. F.; Bird, R. B. *Molecular Theory of Gases and Liquids*; John Wiley & Sons: New York, 1964; Chapter 7.

(9) Slattery, J. C. *Momentum, Energy and Mass Transfer in Continua*; McGraw-Hill Book Company: New York, 1972; pp 472−478.

(10) Krishna, R.; Wesselingh, J. A. The Maxwell−Stefan Approach to Mass Transfer. *Chem. Eng. Sci.* **1997**, *52* (6), 861−911.

(11) Reid, R. C.; Prausnitz, J. M.; Sherwood, T. K. *The Properties of Gases and Liquids*, 3rd ed.; McGraw-Hill Book Company: New York, 1977; pp 547−548.

(12) Schmidt, T.; Leshchyshyn, T. H.; Puttagunta, V. R. Diffusivity of CO_2 into Reservoir Fluids. 33rd Annual Technical Meeting of the Petroleum Society of CIM, Calgary, Canada, June 6−9, 1982; Paper 82-33-100.

(13) Renner, T. A. Measurement and Correlation of Diffusion Coefficients for CO_2 and Rich-Gas Applications. *SPE Reservoir Eng.* **1988**, May, 517−523.

(14) Riazi, M. R. A New Method for Experimental Measurement of Diffusion Coefficients in Reservoir Fluids. *J. Pet. Sci. Eng.* **1996**, *14*, 235−250.

(15) Fu, B. C. H.; Phillips, C. R. New Technique for Determination of Diffusivities of Volatile Hydrocarbons in Semi-Solid Bitumen. *Fuel* **1979**, *58*, 557−560.

(16) Das, S. K.; Butler, R. M. Diffusion Coefficients of Propane and Butane in Peace River Bitumen. *Can. J. Chem. Eng.* **1996**, *74*, 985−992.

(17) Yu, C. S. L. The Time-Dependent Diffusion of CO_2 in Normal-Hexadecane at Elevated Pressures. M.Sc. Thesis, University of Calgary, Calgary, Canada, 1984.

(18) Woessner, D. E.; Snowden, B. S., Jr.; George, R. A.; Melrose, J. C. Dense Gas Diffusion Coefficients for the Methane−Propane System. *Ind. Eng. Chem. Fundam.* **1969**, *8* (4), 779−786.

(19) Zhang, Y.; Maini, B.; Hyndman, C. L. Measurement of Gas Diffusivity in Heavy Oils. 49th Annual Technical Meeting of the Petroleum Society of CIM, June 8−10, 1998, Calgary, Canada; Paper 98−63.

(20) Nyugen, T. A.; Farouq Ali, S. M. Effect of Nitrogen on the Solubility and Diffusivity of Carbon Dioxide into Oil and Oil Recovery by the Immiscible WAG Process. *J. Can. Pet. Technol.* **1998**, *37* (2), 24−31.

(21) Mehrotra, A. K.; Garg, A.; Svrcek, W. Y. Prediction of Mass Diffusivity of CO_2 into Bitumen. *Can. J. Chem. Eng.* **1987**, *65*, 826−832.

(22) Upreti, S. R.; Mehrotra, A. K. Simulation of Constant Temperature Ethane Diffusion in Bitumen: Groundwork for Experimental Measurement of Diffusivity. In *Engineering the Future for Human Well-Being*; Nath, S., Ed.; Indian Institute of Chemical Engineers: New Delhi, India, 1998; IIChE Golden Jubilee Congress, New Delhi, India, Dec 14−18, 1997; Vol. 2, pp 966−975.

(23) Courant, R.; Hilbert, D. *Methods of Mathematical Physics*; Interscience Publishers: New York, 1953; Vol. 1, pp 221−222.

(24) Vargaftik, N. B. *Handbook of Physical Properties of Liquids and Gases: Pure Substances and Mixtures*, 2nd ed.; Hemisphere Pub. Corp.: New York, 1975.

(25) Stoer, J.; Bulirsch, R. *Introduction to Numerical Analysis*; Springer-Verlag: New York, 1980.

(26) Press: W. H.; Teukolsky, S. A.; Vetterling, W. T.; Flannery, B. P. *Numerical Recipes in C: The Art of Scientific Computing*, 2nd ed.; Cambridge University Press: New York, 1995; pp 724−732.

(27) Fletcher, R.; Reeves, C. M. Function Minimization by Conjugate Gradients. *Comput. J.* **1964**, *7* (2), 149−154.

Received for review August 24, 1999
Revised manuscript received January 6, 2000
Accepted January 13, 2000
IE990635A